Available online at www.sciencedirect.com
SCIENCE DIRECT®
C. R. Physique 4 (2003) 475–487
COMPTES RENDUS PHYSIQUE

Exotic nuclei/Les noyaux exotiques

Molecules in nuclei

Martin Freer

School of Physics and Astronomy, University of Birmingham, Edgbaston, Birmingham, B15 2TT, UK

Presented by Guy Laval

Abstract

The possible existence of analogues of atomic molecules within nuclei is considered in the context of the neutron-rich beryllium and carbon isotopes, where the underlying α cluster structure is believed to produce a multi-centred potential in which valence neutrons move. The generation of molecular wave-functions is examined and the link with the deformed harmonic oscillator and the Nilsson single-particle level scheme traced. Experimental evidence for the existence of molecular exotic cluster structures is reviewed particularly the nature of spectroscopic information provided by break-up reaction measurements. ***To cite this article: M. Freer, C. R. Physique 4 (2003).***

Résumé

Noyaux moléculaires. Les noyaux riches en neutrons semblent présenter des états analogues aux molécules atomiques. En particulier, une sous-strucuture en particules α de noyaux légers riches en neutrons tels les Bérylium et des Carbones pourrait créer un potentiel à plusieurs centres piègeant des neutrons de valence. Cet article fait le point sur les fonctions d'onde de ces états moléculaires et sur leur lien avec les orbites de Nilson et de l'oscillateur harmonique déformé. Les preuves expérimentales de l'existence d'états nucléaires agréés en molécules est passé en revue avec un point particulier sur les informations spectroscopiques provenant de la mesure de leur canaux de désintégration. ***Pour citer cet article : M. Freer, C. R. Physique 4 (2003).***

Keywords: Nuclear molecules; Light neutron-rich nuclei; Break-up reactions

Mots-clés : Noyaux moléculaires ; Noyaux légers riches en neutrons ; Canaux de désintégration

1. Clustering and molecules

Clustering has long been known to play an influential role in the structure of nuclei, ever since the first observations of α-decay, which appeared to require that such particles were preformed within the nucleus. Presently, even more exotic decay modes are known following on from the pioneering work of Rose and Jones with the observation of ^{14}C decay of ^{223}Ra [1], rather than α-emission, suggesting even more complex clusters might pre-exist in heavy nuclei.

In light nuclei it is predicted that it should be possible for the nucleus to condense into its full α-particle structure. Ikeda [2] boldly conjectured that the appearance of clustering should be strongly correlated with the cluster decay thresholds. That is, when a cluster decay threshold is approached then the cluster structure should be manifest. So, for example, the ^{8}Be nucleus, which is the simplest α–α cluster system and is indeed unbound to α-decay even in the ground state, would be expected to exhibit a pronounced two-α cluster structure. It transpires that the reduced width for α-decay and the rotational characteristics of this nucleus strongly support the theoretical speculation. Similarly, the cluster structures of ^{16}O and ^{20}Ne are well documented,

E-mail address: M.Freer@bham.ac.uk (M. Freer).

1631-0705/03/$ – see front matter
doi:10.1016/S1631-0705(03)00050-1

for example, close to the α-decay threshold ^{20}Ne displays a strong α-^{16}O cluster behavior which, owing to its asymmetry, displays octupole behaviour [3]. Similarly at slightly higher energies there are bands in this nucleus which are identified with ^{12}C–^{8}Be clustering [4]. ^{12}C, on the other hand, has strongly resisted efforts to obtain a detailed understanding of its structure. The ground state is indeed compact, in agreement with Ikeda's picture and in cluster models is associated with a triangular configuration of α-particles [5,6]. However, the 7.65 MeV (0^+) *Hoyle resonance* which was suggested by Ikeda to correspond to the linear chain structure of α-particles, appears not to possess such a structure. Indeed, present theoretical analysis indicates that this state may be linked with a dilute 3-α particle state with properties reminiscent of a Bose gas [7]. Although the state appears to possess a cluster content the location of the 3α chain configuration remains something of a mystery.

Nevertheless, the cluster structure present in these nuclei has a marked impact on their energy level spectrum and transition probabilities between levels. Indeed, it is not possible to find an accurate description within the single-particle framework of the shell model. It is also known that clustering is present in systems which do not entirely decompose into α-particle subunits, for example ^{6,7}Li possess $\alpha + \mathrm{d}$ and $\alpha - \mathrm{t}$ cluster structures. Thus, it might be anticipated that the clustering present, for example in ^{8}Be, has a determining role to play in the structural properties of heavier $N \neq Z$ isotopes, e.g., ^{9,10,11,12,14}Be. Indeed, the cluster–cluster potential in which the valence neutrons move should introduce molecular characteristics for the valence particle wave-functions.

In covalent atomic molecules electrons are *exchanged* between charged nuclei, and the molecular wave-functions, ψ, approximately correspond to Linear Combinations of Atomic Orbitals (LCAO), χ_i,

$$\psi = c_1\chi_1 + c_2\chi_2 + c_3\chi_3 + \cdots + c_n\chi_n. \tag{1}$$

This ensures that, in the limit that the electron lies close to the nucleus, the orbit is close to being that of the atomic orbit. In order that linear combinations produce bound atomic molecules, the energies of the atomic orbits must be similar, they should maximally overlap and they must possess common symmetry properties. This condition is clearly satisfied for symmetric molecules, e.g., H_2. It is intriguing that the clusterisation of the nuclear potential in beryllium nuclei could lead to similar effects, where the neutrons can reside in linear combinations of nuclear orbits, in particular where the cores are identical α-particles as is the case for α-conjugate nuclei.

2. Deformed oscillator and clustering

As a guide to the structure of the beryllium isotopes and location of molecular orbits the deformed harmonic oscillator (HO) is a useful illustration. The energy level scheme of the deformed oscillator is given in Fig. 1. Important for ^{8}Be is the break in degeneracy that occurs for the $N = 1$ shell with increasing deformation along the z-axis. The oscillator level $(n_x, n_y, n_z) = (0, 0, 1)$ falls with deformation, corresponding to the decrease in oscillation frequency with increasing deformation, whereas the two levels $(1, 0, 0)$ and $(0, 1, 0)$ rise, remaining degenerate. Thus, at a deformation of $2:1$, commensurate with the cluster character, the oscillator levels $(0, 0, 0)$ and $(0, 0, 1)$ should be fully occupied. As a consequence, the valence neutrons in the neutron-rich Be isotopes should then reside within the orbits $(1, 0, 0)$ and $(0, 1, 0)$, i.e., up to a maximum of 4, and the $(0, 0, 2)$ level. The 6 valence neutrons would thus close the second deformed shell which would correspond to the nucleus ^{14}Be. Thus, for this particular nucleus, both the core and the valence neutrons would possess a tendency to be deformed. Note, this picture already indicates that the $N = 1$ and $N = 2$ orbits are degenerate at $2:1$, as has been experimentally observed for the Be isotopes [8]. As an aside, it should be recognised that the harmonic oscillator possesses symmetries which are closely related to the appearance of clustering. It can be observed that the pattern of degeneracies which appear for the undeformed potential, namely 2, 6, 12, ..., are repeated twice at a deformation of $2:1$ and three times at $3:1$, etc. It is also noticeable that the separation between the 2 and 6 degeneracy level crossings increases at $2:1$ and even more so at $3:1$. Thus, the level scheme is such that it is possible to view the structure at $2:1$ as arising from two smaller HO potentials and at $3:1$, three potentials. These patterns and symmetries have been explored in detail by Nazarewicz and Dobaczewski [9] and in reference [10].

Given that the HO possess multi-centred symmetries, the wave-functions shown in Fig. 1, should possess similar symmetries. The link with the molecular degree of freedom can be explored by constructing the wave-functions from their multi-centred counterparts using the linear combination approach. In atomic physics the Hückel Molecular Orbital approach provides a rather elegant method for the evaluation of molecular orbits.

3. The Hückel method

Consider a two centre problem, where following from Eq. (1) the molecular wave-function can be written as

$$\psi = c_1\chi_1 + c_2\chi_2, \tag{2}$$

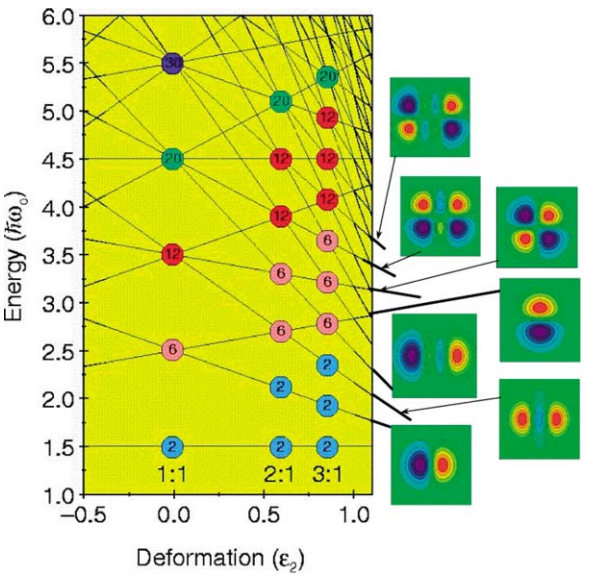

Fig. 1. The energy levels of the deformed harmonic oscillator. The degeneracies that appear in the energy levels at integer ratios of axial deformations, e.g., 2 : 1, 3 : 1, etc. are indicated by the numbers in the circles. It is clear that the pattern of degeneracies found for the spherical oscillator are repeated twice at 2 : 1 and three times at a deformation of 3 : 1. Also shown are the amplitudes of the oscillator wave-functions plotted in the x–z plane for the $(n_x, n_y, n_z) = (0, 0, 1)$, $(0, 0, 2)$, $(1, 0, 0)$, $(1, 0, 1)$, $(1, 0, 2)$ and $(1, 0, 3)$ levels, in order of increasing energy of the levels on the right-hand side of the plot.

where the coefficients c_1 and c_2 and the energies of the orbit are to be determined. Now the wave-function ψ must satisfy

$$H\psi = E\psi. \tag{3}$$

Given ψ, it is possible to calculate E from

$$E = \frac{\int \psi^* H \psi \, \mathrm{d}\tau}{\int \psi^* \psi \, \mathrm{d}\tau}. \tag{4}$$

However, if ψ is unknown then a variational technique must be employed to calculate the optimal energy E via variation of the constants c_1 and c_2. These considerations lead to the *secular* determinant

$$\begin{vmatrix} H_{11} - E & H_{12} - E \cdot S_{12} \\ H_{12} - E \cdot S_{12} & H_{22} - E \end{vmatrix} = 0. \tag{5}$$

Here

$$H_{12} = \int \chi_1^* H \chi_2 \, \mathrm{d}\tau = \int \chi_2^* H \chi_1 \, \mathrm{d}\tau, \tag{6}$$

$$H_{11} = \int \chi_1^* H \chi_1 \, \mathrm{d}\tau, \tag{7}$$

$$H_{22} = \int \chi_2^* H \chi_2 \, \mathrm{d}\tau, \tag{8}$$

$$S_{12} = \int \chi_1^* \chi_2 \, \mathrm{d}\tau = \int \chi_2^* \chi_1 \, \mathrm{d}\tau. \tag{9}$$

$H_{11} = H_{22}$ is called α which is simply the Coulomb integral, and H_{12} is the resonance integral called β, hence

$$\begin{vmatrix} \alpha - E & \beta - E \cdot S_{12} \\ \beta - E \cdot S_{12} & \alpha - E \end{vmatrix} = 0. \tag{10}$$

This approach assumes that the overlap of atomic orbits between neighbouring atoms is zero, i.e., $S_{12} = 0$ and conversely $S_{11} = 1$. Importantly for more complex systems H_{ij} is assumed to be zero if the atoms are not directly bonded to each other. So dividing through by β and setting $x = (\alpha - E)/\beta$ we get

$$\begin{vmatrix} x & 1 \\ 1 & x \end{vmatrix} = 0. \tag{11}$$

The solution to this is clearly $x = \pm 1$ and thus $E = \alpha \pm \beta$, and the corresponding wave-functions are

$$\psi_1 = \frac{1}{\sqrt{2}}(\chi_1 + \chi_2), \qquad E = \alpha + \beta, \tag{12}$$

$$\psi_2 = \frac{1}{\sqrt{2}}(\chi_1 - \chi_2), \qquad E = \alpha - \beta. \tag{13}$$

Clearly, the state associated with ψ_1 lies 2β higher in energy than that associated with ψ_2.

3.1. Link to nuclear molecules and the deformed Harmonic Oscillator

This perhaps unsurprising result was also arrived at by Harvey [11], in the treatment of clustering in the nucleus ^{8}Be, seminal work which gave rise to the *Harvey prescription*. In the present case the valence neutrons of the isotopes $^{9-14}$Be would occupy harmonic oscillator orbits $(1,0,0)$, $(0,1,0)$ and $(0,0,2)$. For ^{9}Be in the molecular picture the two-centre orbits would be constructed from linear combinations of the orbits available to the neutron in ^{5}He namely $(1,0,0)$, $(0,1,0)$ and $(0,0,1)$. Fig. 2 shows the linear combinations corresponding to Eqs. (12) and (13) for the $(1,0,0)$ and $(0,0,1)$ HO wave-functions evaluated in the $z{-}x$ plane. Fig. 2(b) shows the case for Eq. (13) and 2(c) Eq. (12) for the $(1,0,0)$ wave-function. The presence of the additional node is associated with the higher energy configuration. The lowest energy orbit would correspond to the bonding case (π-bond) whilst the higher energy counterpart is the anti-bonding orbit. Figs. 2(e) and 2(f) show the results for the $(0,0,1)$ orbits which give rise to (e) bonding (σ-bond) and (f) anti-bonding wave-functions. It is clear that analogues of these wave-functions can be found in the HO wave-functions as illustrated in Fig. 1. Fig. 2(b), is analogous to the $(1,0,0)$ wave-function, 2(c) to $(1,0,1)$, 2(e) to $(0,0,2)$ and finally 2(f) to $(0,0,3)$. Clearly, as illustrated in Eqs. (12) and (13) and accentuated in the *Harvey rules* [11], the molecular wave-functions are formed in accordance with the behaviour of the n_z quantum numbers of the original orbits from which the molecular orbits were formed, such that $N_z = 2n_z$ and $N_z = 2n_z + 1$, where N_z is the HO quantum number of the orbit linked to the molecular wave-function. In this manner, it is possible to identify orbits in the deformed HO at a deformation of 2 : 1 which have molecular character. It is clear that those most readily available to the valence neutrons in the beryllium isotopes are those labeled as σ and π-bonds above.

3.2. Three-centre systems

There is a natural extension both on the atomic and nuclear scales to more complex molecular systems. Once again following the Hückel method, for a three centre system the secular determinant becomes

$$\begin{vmatrix} x & 1 & 0 \\ 1 & x & 1 \\ 0 & 1 & x \end{vmatrix} = 0 \tag{14}$$

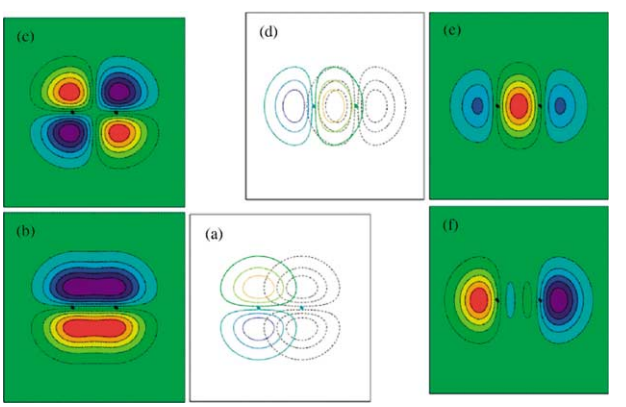

Fig. 2. Molecular wave-functions contructed from HO $(n_x, n_y, n_z) = (1,0,0)$ and $(0,0,1)$ orbits. (a) shows the overlap of the two individual wave-functions and (b) and (c) the result of forming linear combinations in accord with Eqs. (12) and (13). The result shown in (b) corresponds to the π-bond. Again, (d) is the overlap of the two $(0,0,1)$ orbits and (e) and (f) the two linear combinations. Orbit (e) corresponds to the σ-bond configuration.

if the three centres are co-linear, or if they form an equilateral triangular structure then the determinant has the form

$$\begin{vmatrix} x & 1 & 1 \\ 1 & x & 1 \\ 1 & 1 & x \end{vmatrix} = 0, \tag{15}$$

where the non-zero terms ensure the overlap of the molecular wave-functions of the first and third centre. The solutions of these two equations lead to the roots $x = -\sqrt{2}, 0, \sqrt{2}$ for the first determinant and $x = -2, 1, 1$ for the other. Remembering $x = (\alpha - E)/\beta$ this implies three energy levels split by $\sqrt{2}\beta$ in the first case and 2β and 0 (i.e., two degenerate solutions) in the second. The coefficients of the one-centred wave-functions, χ_i, for the three roots (as in Eq. (1)) can be simply computed from

$$c_i = \frac{Co_i(root)}{\sum_{n=1}^{3} Co_n(root)}, \tag{16}$$

where $Co_i(root)$ are the three cofactors of the above determinants evaluated at the three roots. This produces the three wave-functions for the co-linear configuration

$$\psi_1 = \frac{1}{2}\chi_1 + \frac{1}{\sqrt{2}}\chi_2 + \frac{1}{2}\chi_3, \tag{17}$$

$$\psi_2 = -\frac{1}{\sqrt{2}}\chi_1 + \frac{1}{\sqrt{2}}\chi_3, \tag{18}$$

$$\psi_3 = \frac{1}{2}\chi_1 - \frac{1}{\sqrt{2}}\chi_2 + \frac{1}{2}\chi_3 \tag{19}$$

and for the triangular case

$$\psi_1 = -\frac{1}{\sqrt{3}}\chi_1 + \frac{1}{\sqrt{3}}\chi_2 + \frac{1}{\sqrt{3}}\chi_3, \tag{20}$$

$$\psi_2 = -\sqrt{\frac{2}{3}}\chi_1 + \frac{1}{\sqrt{6}}\chi_2 + \frac{1}{\sqrt{6}}\chi_3, \tag{21}$$

$$\psi_3 = \sqrt{\frac{2}{3}}\chi_1 - \frac{1}{\sqrt{6}}\chi_2 - \frac{1}{\sqrt{6}}\chi_3. \tag{22}$$

Now forming the linear combinations of $(1, 0, 0)$ and $(0, 0, 1)$ orbits in turn for the co-linear arrangement produces the wave-functions shown in Figs. 3 and 4. The former leads to π-type configurations, two of which have already been found for the two-centred molecules.

Returning to the harmonic oscillator, but this time examining the level ordering at a deformation of 3 : 1, the sequence above the filling of the three levels $(0, 0, 0)$, $(0, 0, 1)$ and $(0, 0, 2)$ with *α-particles* is $[(1, 0, 0), (0, 1, 0), (0, 0, 3)]$, $[(0, 1, 1), (1, 0, 1), (0, 0, 4)]$ and $[(0, 1, 2), (1, 0, 2), (0, 0, 5)]$ – where square brackets denote degenerate levels.

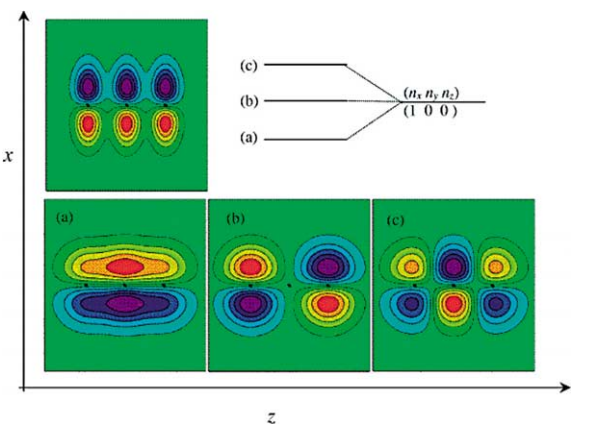

Fig. 3. Molecular wave-functions for three centres for three $(n_x, n_y, n_z) = (1, 0, 0)$ orbits. The uppermost figure shows the three individual orbits before the linear combinations shown in parts (a), (b) and (c) are formed, as described by Eqs. (17), (18) and (19). Again part (a) corresponds to the π-type arrangement. The energy splitting of the three orbits is shown schematically.

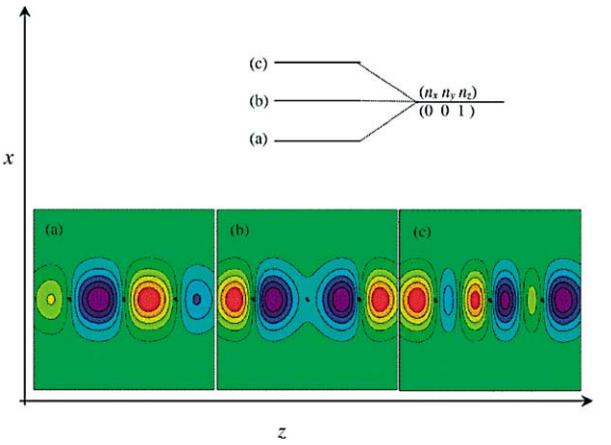

Fig. 4. Molecular wave-functions for three centres for three $(n_x, n_y, n_z) = (0, 0, 1)$ orbits. (a), (b) and (c) are linear combinations associated with Eqs. (17), (18) and (19). Part (a) corresponds to the $(0, 0, 3)$ HO orbit. The energy splitting of the three orbits is shown schematically. The dots indicate the location of the three centres.

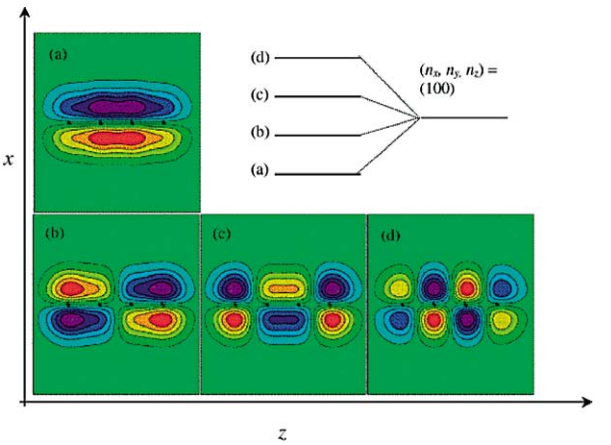

Fig. 5. Molecular wave-functions for four centres based on $(n_x, n_y, n_z) = (0, 0, 1)$ orbits. The same pattern observed in Fig. 3 is found. Again the relative energy splitting of the 4 levels is indicated.

It is clear that the three wave-functions shown in Figs. 3 (a), (b) and (c) correspond to the levels $(1, 0, 0)$, $(1, 0, 1)$ and $(1, 0, 2)$, i.e., one from each deformed shell. More importantly, the extension from the *Harvey rules* of the two-centred system now appear, i.e., the molecular N_z quantum number is related to the original n_z values by $N_z = 3n_z$, $3n_z + 1$, $3n_z + 2$. Similar patterns may be observed in the combinations of the $(0, 0, 1)$ HO orbits to form σ-like three-centred bonds, where broadly the three configurations can be linked with the $(0, 0, 3)$, $(0, 0, 4)$ and $(0, 0, 5)$ HO orbits.

To complete the picture of chain-like structures the solution of the 4-centre system is shown in Fig. 5 for linear combinations of the $(1, 0, 0)$ orbits. The same pattern is again observed with the lowest energy level being the continuation of the $(1, 0, 0)$ level from 3 : 1 to 4 : 1 deformation, and the higher energy levels possess increasing numbers of nodes along the z-direction.

For the chain-type structures it is possible to make some general observations: (i) the lowest energy, and thus dominant π-molecular bond corresponds to the extension of the $(1, 0, 0)$ and $(0, 1, 0)$ levels from the $N = 1$ shell, and it is this orbit which will contribute to the lowest energy π-bond for all chain-lengths. These levels may be linked to the $[1, 0, 1]3/2^-$ Nilsson level. (ii) the lowest energy σ-type level for linear structures will correspond to the $(0, 0, N)$ HO level where N is the number of α-particles in the chain, these levels correspond to the Nilsson orbits $[N, N, 0]1/2^{\pi}$, $\pi = (-1)^N$.

3.3. Two-dimensional structures

As indicated it is possible to apply the Hückel method to two-dimensional structures (the benzene molecule is rather an elegant example). Fig. 6 shows the three wave-functions for the triangular arrangement of three α-particles for a linear

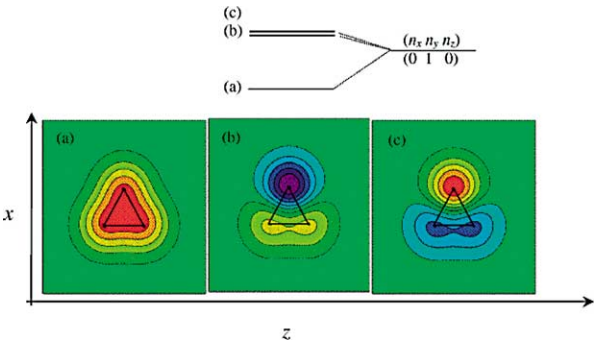

Fig. 6. Two dimensional molecules. The molecular wave-functions for 3 $(n_x, n_y, n_z) = (0, 1, 0)$ produced using Eqs. (20), (21) and (22). The three centres are indicated by the triangle. (a) correponds to nucleons/electrons delocalised above and below the plane of the triangle, with a change of sign in crossing the plane. (b) and (c) correspond to degenerate orbits, they are the same apart from a change in sign.

combination of three $(0, 1, 0)$ orbits, i.e., with the oscillation quantum perpendicular to the plane of the triangle. For the lowest energy mode the wave-function is delocalised above and below the plane. The other two orbits (which incidentally due to the symmetry of the triangle would be unchanged by rotations of $\pi/3$) possess a single radial node (or nodes around the ring), and the energy degeneracy becomes clear from the figure. Extensions to more centres leads to similar patterns with increasing numbers of nodes cyclically.

As with the linear chain structures it is also possible to make some general statements for the two-dimensional states. The lowest energy bonds (considering π-character only) correspond to the HO level $(0, 0, 1)$ in Fig. 1 extrapolated to oblate deformations, where it becomes perpendicular to the plane of deformation for oblate nuclei. Just as on the prolate side the $(1, 0, 0)$ and $(0, 1, 0)$ levels are the dominant molecular orbitals the $(1, 0, 0)$ level fulfills the same role on the oblate side. The higher nodal partners will correspond to linear combinations of the $(0, 1, 1) + (1, 0, 1)$, $(0, 2, 1) + (2, 0, 1)$ levels etc.

To conclude, it is possible to link directly the Hückle molecular wave-functions with the energy levels in the deformed oscillator and thus their counterparts in the Nilsson model. As a result it is possible to predict which Nilsson orbits play an important role in the formation of nuclear molecules, and thus for which nuclei and excitation energies the states should appear.

4. Links with nuclear models

The presence of molecular symmetries in the deformed harmonic oscillator indicates that more rigorous treatments of nuclei should possess similar traits. The Antisymmeterised Molecular Dynamics (AMD) framework, provides a description of the nucleus in terms of the interactions of A nucleonic (Gaussian) wave-packets combined via a Slater determinant. In principle this model allows the energy of the system to be probed as a function of the nucleon coordinates, and has no intrinsic predilection for clusterisation. This model has been used extensively to describe the structure of light nuclei and has met with a remarkable degree of success [12–16]. In particular the model reveals the molecular characteristics of the ground state of ^{10}Be in terms of the predicted π^2 character, and suggests the existence of a deformed band based on a σ^2 configuration at $\sim$8 MeV [13,14]. This model has also been extended to the more exotic neutron rich isotopes ^{11}Be [15] and ^{12,14}Be [16], where once again evidence for molecular, exotic cluster, structures are suggested. The molecular-orbital (MO) prescription results also coincide with those of the AMD description of ^{10}Be [17]. Here the molecular structure is an explicit part of the model, molecular orbits of neutrons are created, much as described in Section 3, by forming linear combinations of single-centre orbits based on α-particle cores. Nevertheless, it is interesting that such calculations verify that the ground state of ^{10}Be should be π in character and the 0_2^+ state possess neutrons in σ molecular orbits. The generator coordinate method (GCM) also finds cluster bands in the beryllium isotopes, e.g., in ^{12}Be [18]. So the picture which emerges from these numerous, and various, theoretical approaches is one in which molecular wave-functions should play an important role in the two-centre systems. Albeit a universal feature of these calculations, the final judgment will be experimental.

5. Experimental evidence for molecules

In this section the experimental evidence for the existence of molecular structures in beryllium isotopes is considered, with a particular emphasis on the use of break-up reactions as an experimental probe of such exotic structures.

5.1. ^{9}Be

The nucleus ^{9}Be possesses an interesting character, it is Borromean in nature, meaning that none of the two-body subsystems, ^{8}Be or ^{5}He, are bound. The ground state has $J^{\pi} = 3/2^{-}$, and there are two more low excitation states which play an important role in the structure of this nucleus these are a $1/2^{+}$ state at 1.68 MeV and $1/2^{-}$ at 2.78 MeV. It is particularly interesting that the $1/2^{+}$ state should lie so close to the ground state as it implies that orbits from the s–d shell play an important role in the character of this nucleus. As indicated in Fig. 1 levels from the $N = 2$ shell can be lowered in energy for deformed systems, in particular that linked with the $[1, 1, 0]1/2^{+}$ Nilsson orbit. This points to two observations, the first is that ^{9}Be must possess significant deformation and the second is that the $1/2^{+}$ state is linked with an orbit which has already been found to possess a σ-bond molecular character. The ground state conversely possesses a single neutron in a Nilsson orbit which was shown to possess π-type characteristics. Fig. 7 shows the energy-spin systematics for this nucleus [19–21]. There is a clear rotational band based upon the ground state, and the extracted moment of inertia demonstrates that indeed the nucleus is elongated with a deformation commensurate with that of ^{8}Be, i.e., an axis ratio of close to 2 : 1. There is indeed a rotational band corresponding to the $1/2^{+}$ state also, however the corriolis decoupling effect characteristic of $K = 1/2$ bands is evident. Nevertheless, the extracted rotational behaviour suggests again a deformed nucleus. ^{9}Be is bound against neutron decay by only 1.66 MeV, if the neutron is removed then the remaining constituents dissociate, just as with the H_2^+ molecule when the single electron is detached. Thus, in many senses the nucleus ^{9}Be is a nuclear molecule. A detailed analysis of the molecular properties of this nucleus and of other beryllium isotopes is presented in reference [19–21]. As a note of caution, as shown in Fig. 7 several of the states in ^{9}Be remain to have spins firmly assigned by direct measurements. This is an important next step.

A different picture emerges for the proton-rich nucleus ^{9}B. ^{9}B is particle unbound in the ground state, and thus the stabilising influence of the neutron in ^{9}Be is not found for a molecular proton. Moreover, the $1/2^{+}$ isobaric analogue of the 1.68 MeV state in ^{9}Be has proven extremely difficult to locate [23], linked to its large width, again an indication that in both σ and π orbits the Coulomb repulsion more than outweighs the gain in energy from the formation of the molecular state. As consequence, the majority of experimental and theoretical interests have been directed towards the neutron-rich isotopes.

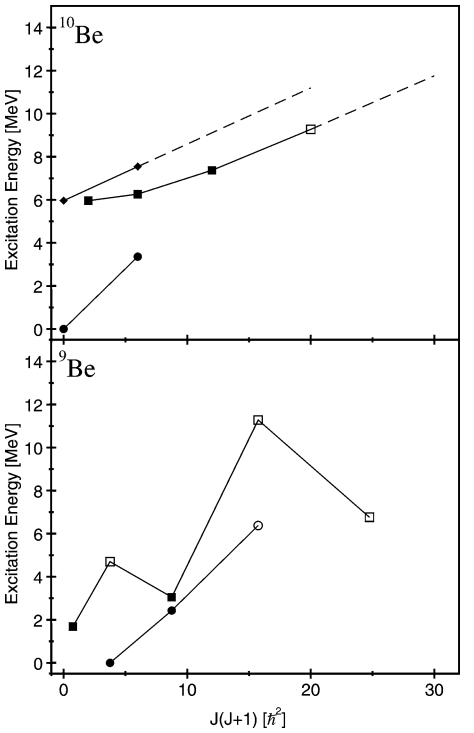

Fig. 7. The energy-spin systematics for the nuclei ^{9}Be and ^{10}Be. States with firm spin and parity assignments are represented by filled symbols, whilst open symbols indicate tentative assignments. The assignments are taken from [22]. For ^{9}Be there appear to be two rotational bands, one based on the $3/2^{-}$ ground state (circles) and the other the $1/2^{+}$ excited state (squares). For ^{10}Be there are three possible bands (i) based on the ground state (circles), (ii) a negative parity band based on the 1^{-} state (squares) and (iii) a positive parity band from the 0_2^+ excited state (diamonds). The possible extensions of the bands are indicated by the dashed lines. It is clear that for both nuclei there are a number of spin and parity assignments required for a full description of the rotational behaviour.

The progression towards a deeper understanding of molecules via either the addition of more neutrons, or more centres has been steady, but much remains to be understood before these more complex systems may be conclusively referred to as 'molecules'.

5.2. ^{10}Be

Given the ground state structure of ^{9}Be, the ground state of ^{10}Be should be π^2, and this is certainly the picture which also emerges from the AMD calculations [13,14]. The ground state is bound by 6.8 MeV against neutron decay, and by 7.4 MeV for α-decay. Thus the cluster/molecular structure is less obvious here. The σ^2 configuration on the other hand, according to the expectations of the AMD picture, lies close to these decay thresholds. Moreover, as the σ-neutrons intercede between the two α-cores then via the Pauli-principle the cores are forced to larger separations, and thus the molecular structures should be more visible in this instance. The 6.18 MeV, 0^+ state, and the 7.54 MeV 2^+ state have been suggested [19–21] to be the first two members of the molecular band. However, if these are rotational states then there should be a 4^+ member of the band, which lies between 10 and 12 MeV.

The study of the spectroscopy of nuclei above particle decay thresholds is intensely difficult, often resolution is limited by experimental considerations and the extraction of spin information is at best model dependent and at worst impossible due to the featureless nature of angular distributions in heavy-ion reactions. However, break-up reactions do provide a possible solution. In such measurements the resonant particle of interest may be excited via inelastic scattering or transfer. In the case of ^{10}Be the ^{7}Li(^{7}Li,^{10}Be)α reaction has been used with great effect [24,25]. The decay of the resonant particle, in this case ^{10}Be, into the cluster components may then be used as a possible indicator of cluster structure – states possessing large reduced widths for cluster decay should appear most strongly in the decay spectrum. The reconstruction of the emission angles of the two break-up fragments, in the case of ^{10}Be this would be $^{6}\mathrm{He} + \alpha$, using position sensitive detectors permits the reconstruction of the excitation energy of the decaying state and a measurement of the angular distributions with which the decay process proceeds. The resolution with which the excitation energy may be reconstructed is determined largely by the position resolution of the detectors and the angular straggling in the target. With optimal conditions, e.g., 0.1 mm position resolution that can be offered by large area position-sensitive silicon detectors and thin targets energy resolutions of $\leqslant$100 keV are possible.

This experimental approach has been used to study the decay of ^{10}Be into $^{4}\mathrm{He} + {}^{6}\mathrm{He}$ and $^{9}\mathrm{Be} + n$ [24,25]. These measurements find evidence for a state at 10.2 MeV which decays strongly by α-emission compared with neutron decay, which would make it an excellent candidate for the 4^+ member of the σ-band. However, and somewhat disappointingly from the perspective of the molecular interpretation, the state would appear to possess a spin and parity of 3^-. The location of the projected 4^+ state remains something of a mystery as a consequence, and indeed an experimental challenge. Nevertheless, measurements of the partial α-decay width of the 7.54 MeV (2^+) state [26] do show that this state possesses a significant α-cluster component to its wave-function.

It is of course also possible to form molecular configurations from combinations of σ and π-like neutrons. This would correspond to the 1^- band which extrapolates to a band head energy of 5.96 MeV. To date only the first three members of this putative band are known, and the remaining candidates must be fixed in order that the molecular character of this nucleus can be sealed.

To summarise, the case for the molecular structure of ^{10}Be is by no means as clear cut as for ^{9}Be and much remains to be done to fully determine the spectroscopy of this nucleus. Nevertheless, the circumstantial evidence to date suggests that this is a nucleus which *is* molecular in nature.

5.3. ^{12}Be and ^{14}Be

The study of nuclei such as ^{11}Be using break-up reactions is a significant challenge as the main cluster decay channels ($^{6}\mathrm{He} + {}^{5}\mathrm{He}$ and $^{7}\mathrm{He} + {}^{4}\mathrm{He}$) produce nuclei in neutron unbound states which demands the detection of the break-up neutrons for full reconstruction of the decay process. It is possible to infer the neutron momentum from detection of the recoil particle, but this is often another experimental challenge. ^{12}Be on the other hand potentially decays into $^{6}\mathrm{He} + {}^{6}\mathrm{He}$ or $^{8}\mathrm{He} + {}^{4}\mathrm{He}$, with the symmetric decay channel selecting only even spin states since the decay proceeds via two identical spin zero nuclei. The problem with the study of such neutron-rich nuclei is that they require rather exotic reactions to populate them, i.e., negative Q-values and small cross sections which conversely imply large backgrounds. Studies using radioactive beams, however, present much lower backgrounds which more than compensate for the much weaker beam intensities. A beam of ^{12}Be nuclei, which may be inelastically excited into the break-up/$\alpha + 4n + \alpha$ molecular states must be produced via the fragmentation process, extraction of Be from ISOL targets is prohibitively difficult owing to the reactive nature of the element. Typical of fragmentation beams is a rather large energy spread of the products if beam intensity is optimised. So, for example, for the LISE3 separator at GANIL, for a 370 MeV ^{12}Be the spread in energy of the secondary beam is $\sim$18 MeV. Of course it is possible to reduce this uncertainty using time-of-flight techniques to the point where energy loss in the necessarily thick targets becomes an important

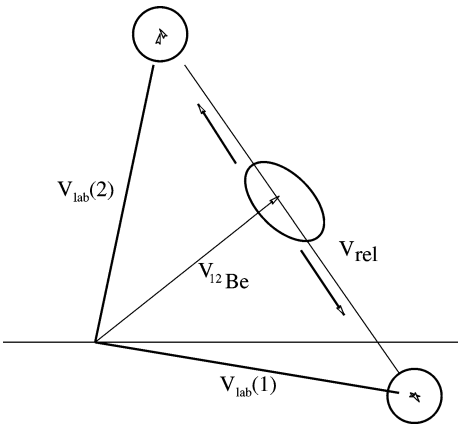

Fig. 8. The vector diagram of the decay of a resonant ^{12}Be nucleus into two ^{6}He nuclei. The vectors $\mathbf{V}_{\rm lab}(1)$ and $\mathbf{V}_{\rm lab}(2)$ are equal to $\mathbf{V}_{^{12}\rm Be} \pm \mathbf{V}_{\rm rel}/2$. The inverse calculation of $\mathbf{V}_{\rm rel}$ does not depend on $\mathbf{V}_{^{12}\rm Be}$.

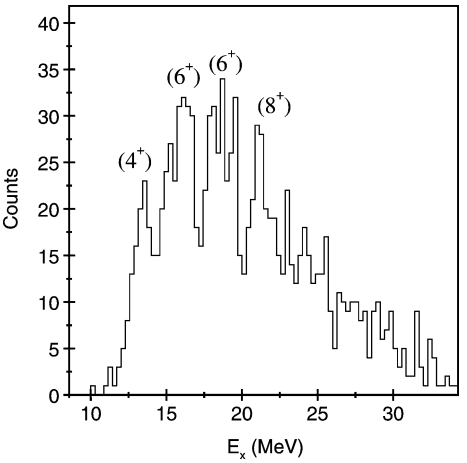

Fig. 9. The excitation energy spectrum for the decay of ^{12}Be into two ^{6}He nuclei. The numbers in the brackets are the tentative spin and parity assignments [27].

consideration. Nevertheless, it is difficult to perform high resolution spectroscopic measurements under such conditions. With break-up reactions the excitation energy of the resonant particle is calculated from the relative velocity vectors of two detected particles, as shown in Fig. 8. The dominant effects of energy spread in the beam energy and the energy loss of the beam in the target appear in the vector corresponding to the emission of the excited ^{12}Be. The break-up products being lighter and less charged experience less energy and angular straggling. The relative velocity is related to the excitation energy via

$$E_x = E_{\rm thresh} + \frac{1}{2}\mu V_{\rm rel}^2, \tag{23}$$

where $E_{\rm thresh}$ is the threshold decay energy and μ is the reduced mass of the decaying system, and the relative velocity is given by

$$\mathbf{V}_{\rm rel} = \mathbf{V}_{\rm lab}(1) - \mathbf{V}_{\rm lab}(2). \tag{24}$$

Thus, the excitation energy calculation is independent of the beam energy resolution, and is largely limited by the product straggling in the target and position resolution of the detectors. Typically energy resolutions of 500 to 700 keV can be achieved.

Fig. 9 shows the reconstructed excitation energy spectrum for the reactions of ^{12}Be from a composite $(CH_2)_n$ target for decays into ^{6}He + ^{6}He [27,28]. The 700 keV excitation energy resolution permits the identification of groups of states in the excitation energy region 10 to 25 MeV. The measurement of the emission angles also allows some estimate to be made of the angular momenta involved in the decay process via an analysis of the angular distributions. These tentatively point towards a

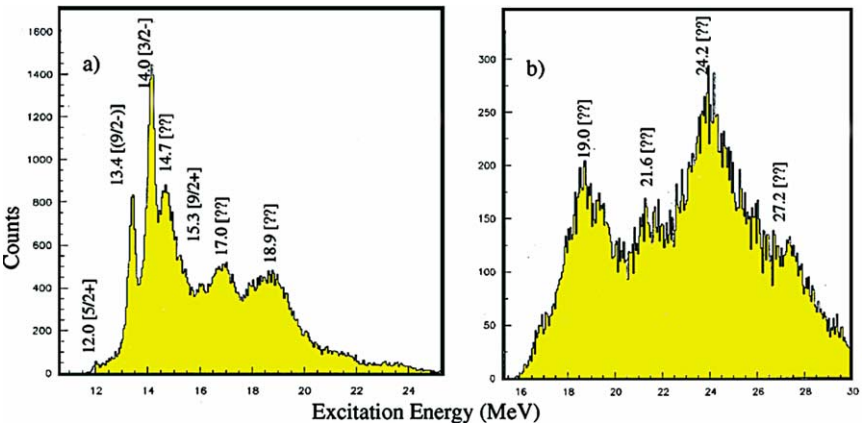

Fig. 10. The excitation energy spectra for the decay of ^{13}C into $\alpha + {}^{9}$Be, as populated in the ^{7}Li(^{9}Be,^{13}C $\rightarrow \alpha + {}^{9}$Be)t break-up reaction. The low excitation and high excitation energy spectra are shown in parts (a) and (b) respectively. The correlation with known states is indicated. Spin and parities are shown in square brackets, [**??**] indicates that spins and parties have not been assigned to the states.

rotational trend for the energies of the excited states. The gradient in turn indicates the decay of a deformed, and perhaps a molecular system.

Such measurements show that the spectroscopy of very neutron-rich nuclei is within experimental capabilities, and provide an indication that exotic cluster structures may be present. Indeed the most neutron-rich Be isotope has recently been studied at the RIKEN radioactive ion-beam facility. Break-up of ^{14}Be into ^{8}He + ^{6}He was observed to proceed from a region of excitation energy above the decay threshold [29]. The excitation energy resolution was limited, however, the spectrum does indicate that the decay proceeds via selected states in this region. Such studies provide considerable promise for the future of this field.

5.4. Three-centre systems, the carbon isotopes

A natural extension of these ideas is to systems composed of more than two centres, i.e., α-chains. Evidence for the 3α chain in ^{12}C is sparse. Historically, the 7.65 MeV (0^+) state has been linked with the chain configuration (see, for example, [6]). However, the lack of experimental evidence for the 2^+ rotational state associated with such a structure has led to the conclusion that the 7.65 MeV state corresponds to an extended triangular structure [30]. The next possible candidate for the chain structure lies some 3 MeV higher in energy at 10.3 MeV (0^+) [31]. However, this resonance is broad and lies in a region of excitation in which detailed spectroscopy of ^{12}C has been difficult. Thus, to date there is no convincing evidence for the existence of the 3α chain-state. The MO calculations of Itagaki for the carbon isotopes [32], may indicate why the chain configuration is unobserved. The calculations suggest that the 3α chain structure in ^{12}C is unstable against the bending mode. However, the same calculations reveal that the addition of valence neutrons helps stabilise the chain structures against bending (a mechanism linked to the Pauli repulsion of the valence neutrons), suggesting that in neutron-rich carbon isotopes molecular chains may exist.

Evidence for the existence of molecular chains in carbon isotopes is in its infancy from the experimental perspective. The HMI group have made some important advances in understanding the structural properties of, for example, ^{13}C and ^{14}C [33]. They find that the states which can be associated either with α-transfer or α-decay reactions fall into two rotational bands, one with positive parity ($3/2^+$ at 11.08 MeV) and the other of negative parity ($3/2^-$ state at 11.75 MeV). These bands possess a moment of inertia which is consistent with a chain-like deformation. However, many of the spins and parities of the states observed in the α-decay spectrum are uncertain, and thus despite being compelling the case is not beyond doubt. Measurements of the α-decay properties of states in for example ^{13}C, in particular angular distributions, are important if the spins of the states in ^{13}C are to be determined. Fig. 10 shows the spectrum of α decaying states observed in the ^{7}Li(^{9}Be,^{13}C $\rightarrow \alpha + {}^{9}$Be)t break-up reaction [34]. A spectrum of states extending from the decay threshold up to ∼28 MeV is clear, and many of these states can be found in the analysis of the ^{13}C spectroscopy performed by Milin. It is hoped that the angular distributions from such data will provide the required spin determinations.

The existence of $\alpha + 2n + \alpha + 2n + \alpha$ states in ^{16}C is predicted by the MO calculations of Itagaki [32]. However, these predictions have yet to be experimentally realised. Measurements of the inelastic break-up of ^{16}C [35] and studies of the $2p$-transfer reactions (^{18}O,^{16}C) using lithium, carbon and oxygen targets [36] have failed to find evidence for such states. The population of molecular states in this system remains a significant challenge.

6. Outlook

The theoretical evidence for molecular structures in beryllium and carbon isotopes is compelling, yet on the experimental front the effect remains to be convincingly demonstrated beyond ^{9}Be. The principle that via the formation of molecular type orbits for valance neutrons which provide stability for the α-chain structures is an exciting prospect. This provides new impetus for the search for exotic chain-like structures in light nuclei. Experiments reporting tentative evidence of α-chains in ^{16}O [37] and ^{24}Mg [38] have largely been unsubstantiated, and the view at present is that such structures have not been observed experimentally. This may be traced, perhaps as indicated by the MO calculations, to the fact that chains are intrinsically unstable against bending, whereas chains augmented by neutrons are not. More broadly, the role of the cluster in neutron rich nuclei is being established, and rather than being diluted by the influence of neutrons diminishing the cluster symmetries, the opposite is true, that the cluster symmetries influence the neutrons. It is possible that these ideas persist to the neutron drip-line, with clustering playing an increasing role in the dissipation of the large imbalance in isospin, i.e., the cluster should be a persistent feature of light drip-line nuclei.

Acknowledgements

I would like to acknowledge the contribution of collaborators from the Charissa and DéMoN collaborations.

References

[1] H.J. Rose, G.A. Jones, Nature 307 (1984) 245.
[2] K. Ikeda, et al., Prog. Phys. Theor. Suppl. Extra No. (1968) 464.
[3] P.A. Butler, W. Nazarewicz, Rev. Mod. Phys. 68 (1996) 349.
[4] D.A. Bromley, Clustering aspects of nuclear structure, in: J.S. Lilley, M.A. Nagarajan (Eds.), 4th International Conference on Clustering Aspects of Nuclear Structure and Nuclear Reactions, 1984, p. 1.
[5] D.M. Brink, in: C. Bloch (Ed.), Proceedings of the International School of Physics, Enrico Fermi, Course XXXVI, Varenna 1965, Academic Press, New York, 1965, p. 247.
[6] N. Takigawa, A. Arima, Nucl. Phys. A 168 (1971) 593.
[7] A. Tohsaki, H. Horiuchi, P. Schuck, G. Röpke, Phys. Rev. Lett. 87 (2001) 192501.
[8] A. Navin, et al., Phys. Rev. Lett. 85 (2000) 266.
[9] W. Nazarewicz, J. Dobaczewski, Phys. Rev. Lett. 68 (1992) 154.
[10] M. Freer, R.R. Betts, A.H. Wuosmaa, Nucl. Phys. A 587 (1995) 36.
[11] M. Harvey, in: Proc. 2nd Int. Conf. on Clustering Phenomena in Nuclei, College Park, USDERA report ORO-4856-26, 1975, p. 549.
[12] Y. Kanada-En'yo, H. Horiuchi, Phys. Rev. C 52 (1995) 647.
[13] Y. Kanada-En'yo, H. Horiuchi, A. Doté, Phys. Rev. C 60 (1999) 064304.
[14] Y. Kanada-En'yo, H. Horiuchi, A. Doté, J. Phys. G 24 (1998) 1499.
[15] Y. Kanada-En'yo, H. Horiuchi, Phys. Rev. C 66 (2002) 024305.
[16] Y. Kanada-En'yo, Phys. Rev. C 66 (2002) 011303.
[17] N. Itagaki, S. Okabe, Phys. Rev. C 61 (2000) 044306.
[18] D. Baye, P. Descouvemont, R. Kamouni, Few Body Systems 29 (2000) 131.
[19] W. von Oertzen, Z. Phys. A 354 (1996) 37.
[20] W. von Oertzen, Z. Phys. A 357 (1997) 355.
[21] W. von Oertzen, Nuovo Cimento 110 (1997) 895.
[22] F. Ajzenberg-Selove, Nucl. Phys. A 490 (1988) 1.
[23] H. Akimune, M. Fujimura, M. Fujiwara, K. Hara, T. Ishikawa, T. Kawabata, H. Utsunomiya, T. Yamagata, K. Yamasaki, M. Yosoik, Phys. Rev. C 64 (2001) 041305.
[24] N. Soić, et al., Europhys. Lett. 34 (1996) 7.
[25] N. Curtis, D.D. Caussyn, N.R. Fletcher, F. Marchal, N. Fay, D. Robson, Phys. Rev. C 64 (2001) 044604.
[26] J.A. Liendo, N. Curtis, D.D. Caussyn, N.R. Fletcher, T. Kurtukian-Nieto, Phys. Rev. C 65 (2002) 034317.
[27] M. Freer, et al., Phys. Rev. Lett. 82 (1999) 295.
[28] M. Freer, Phys. Rev. C 63 (2001) 034301.
[29] A. Saito, et al., RIKEN Accelerator Progress Report 2001, 2002, p. 55.
[30] D.V. Fedorov, A.S. Jensen, Phys. Lett. B 389 (1996) 631.
[31] H. Fynbo, et al., ENAM2001 proceedings to be published in Europhys. Phys. J.
[32] N. Itagaki, et al., Phys. Rev. C 64 (2001) 014301.
[33] M. Milin, et al., contribution to the "Symposium on Nuclear Clusters: from Light Exotic to Superheavy Nuclei", Rauischholzhausen, Germany, 5–9 August, 2002, to be published.

[34] M. Freer, et al., contribution to the "Symposium on Nuclear Clusters: from Light Exotic to Superheavy Nuclei", Rauischholzhausen, Germany, 5–9 August, 2002, to be published.
[35] P.J. Leask, et al., J. Phys. G 27 (2001) 9.
[36] B.J. Greenhalgh, B.R. Fulton, D.L. Watson, N.M. Clarke, L. Donadille, M. Freer, P.J. Leask, W.N. Catford, K.L. Jones, D. Mahboub, Phys. Rev. C 66 (2002) 027302.
[37] P. Chevallier, F. Scheibling, G. Goldring, I. Plesser, M.W. Sachs, Phys. Rev. 160 (1967) 827.
[38] A.H. Wuosmaa, R.R. Betts, B.B. Back, M. Freer, B.G. Glagola, Th. Happ, D.J. Henderson, P. Wilt, I.G. Bearden, Phys. Rev. Lett. 68 (1992) 1295.